Luminescence features of bulk crystals β-$(Ga_xAl_{1-x})_2O_3$

© E.V. Dementeva[1], P.A. Dementev[1], N.P. Korenko[1,2], I.I. Shkarupa[1,2], A.V. Kremleva[2], D.Yu. Panov[2],
V.A. Spiridonov[2], M.V. Zamoryanskaya[1], D.A. Bauman[2], M.A. Odnobludov[2,3], A.E. Romanov[1,2], V.E. Bugrov[2]

[1] Ioffe Institute,
194021 St. Petersburg, Russia
[2] ITMO University,
197101 St. Petersburg, Russia
[3] Peter the Great Saint-Petersburg Polytechnic University,
195251 St. Petersburg, Russia

E-mail: ivanova@mail.ioffe.ru

This work is devoted to the study of the luminescence inhomogeneity nature of bulk $(Ga_xAl_{1-x})_2O_3$ samples grown by the Czochralski method. In the study of sample cleavages by the local cathodoluminescence method, regions with different luminescence were observed. To determine the cathodoluminescence contrast nature, we studied the uniformity of the aluminum distribution, the surface topography, and compared the luminescence spectra and the kinetics of emission bands for different regions of the sample. Also, to determine the luminescence bands nature, the crystal was annealed in air at $1000°C$. This made it possible to observe the change in luminescence for the same region of the sample. Based on the studies performed, it was concluded that inhomogeneous luminescence is associated with the distribution of point defects. Upon annealing in air, the transformation of nonradiative recombination centers into luminescent centers was observed.

Keywords: gallium oxide, luminescence, point defects.

1. Introduction

The interest to crystalline β-Ga_2O_3 arose in early 2000-s, when the first articles about the prospects of its use in various devices were published. Currently there is an increase in number of studies of crystals, nanostructures, nanopowders and epitaxial β-Ga_2O_3 films. High popularity of the material is, on the one hand, due to the high breakdown field value $(8\,MV/cm)$, which makes this material interesting as substrates for power electronics [1,2]. On the other hand, Ga_2O_3 is a large band-gap semiconductor with band gap $4.7-4.9\,eV$, which can be used in optoelectronics. However, the most interesting use of this material are solar-blind photodetectors [2–4]. In this regard, the study of luminescent properties of gallic oxide is of special interest.

Although the practical interest to this material arose relatively recently, the researches of its structure and optical properties, including luminescent ones, have been carried out since the middle of the last century. The wide bands in UV, blue and green spectrum bands were observed in luminescence spectra of gallic oxide. Numerous researches showed, that UV luminescence (UVB) at $\sim 3.1\,eV$ appears in all gallic oxides, regardless of the method for their production. The nature of this band is associated with self-localized excitons [5,6]. The blue band at $\sim 2.65\,eV$ (BB) radiation is observed for doped samples, as well as for undoped ones, but characterizing with high electrical conductivity. The nature of blue band still does not have an unambiguous interpretation. Many authors associate this band with the presence of oxygen vacancies, which determine the electronic conductivity type of undoped gallic oxide [7,8]. Gallic vacancies and formation of oxygen vacancies clusters play and important role in the mechanism of blue radiation band occurrence [9]. The nature of green luminescence at $\sim 2.4\,eV$ (GB) is also still not clear. Liu et al. [10] found the appearance and strengthening of $2.48\,eV$ line upon irradiation of β-Ga_2O_3 with oxygen atoms. The authors, respectively, connected this line with neutral interstitial oxygen impurities. On the other hand, there are theoretical calculations connecting a green $(2.3\,eV)$ band with isolated vacancies V_{Ga}^{2-} (in octahedral position) and V_{Ga}^{1-} (tetrahedral position) [11]. Harwig et al. [12] observed the appearance of only green luminescence when doped with Ga_2O_3 Be^{2+}, as well as together with blue luminescence at doping with Zr^{4+}, Ge^{4+}, Sn^{4+}, Si^{4+} and Li^+. Besides, they showed that annealing of powders in N_2 medium enhances the blue luminescence, while green luminescence enhances upon oxygen annealing. All the above researches confirm the influence of dope additives on the material luminescent properties and connect luminescence bands with point defects of various types.

The solid solution $(Ga_xAl_{1-x})_2O_3$ is of special interest. This may lead to an increase in semiconductor band gap, band shift in the luminescence spectra and the occurrence of new point defect luminescence centers [13]. A study of gallic oxide doped with aluminum by local cathodoluminescence (CL) showed that many of the obtained samples are extremely inhomogeneous with regard to luminescent

properties. The purpose of this study is to study the nature of the luminescent properties inhomogeneity. For this a crystal section with the most inhomogeneous luminescence was selected.

2. Growth method and research methods

The crystals β-(Ga$_x$Al$_{1x}$)$_2$O$_3$ under study were obtained by drawing from the melt by Czochralski method in the growth device „Nika-3" with induction heating (manufactured by FSUE EPSI, Chernogolovka). Powdered Ga$_2$O$_3$ and powdered Al$_2$O$_3$ were used as starting material, reagent purity was 99.999% (5N). To grow crystals, an iridic crucible was used. The crystals were pulled out on a sapphire seed in argon atmosphere Ar — 95% and oxygen O$_2$ — 5% at pressure ~ 1 bar. Details of the technological process were described by us earlier in [14,15]. The grown crystals had a cylindrical shape with a diameter ~ 20 mm and length ~ 15 mm. The reference samples were obtained from crystals by cutting and chipping along the slip planes. The samples β-(Al$_{0.19}$Ga$_{0.81}$)$_2$O$_3$, which were studied by the complex of methods, were received. To study the nature of the cathodoluminescence image contrast, earlier the studied samples were annealed in air. The samples were annealed in a muffle furnace SNOL-4-1300 during 3 hr at 1000°C.

Determination of the samples composition, the study of homogeneous distribution of aluminum, as well as cathodoluminescent researches were carried out on the electron probe microanalyzer CAMEBAX (Cameca) equipped with X-ray and optical spectrometers [16]. In addition the electron probe micro-analyzer allows to get cathodoluminescent images and measure dead time of bands with time resolution $0.3\,\mu$s. Cathodoluminescent images were obtained at an electron beam diameter $150\,\mu$m, electron beam energy 20 keV and 5 keV and current 30 nA. The cathodoluminescence spectra were recorded at the following electron beam parameters: electron energy 20 keV, electron beam current 10 nA and diameter $10\,\mu$m. The composition of the images was determined using electron probe microanalysis method at electron beam energy 20 keV with the use of references Ga$_2$O$_3$ and Al$_2$O$_3$. Available equipment allows to measure the composition and obtain cathodoluminescence spectra in the same area of the sample.

The relief of the investigated samples surface was studied by means of an atomic-force microscope (AFM) Ntegra-Aura (NT-MDT, Zelenograd, Moscow) using standard silicon probes with a specific tip bending radius 7 nm.

The diffraction patterns were obtained by means of X-ray DRON-8 installation in a slot configuration with a fine-focus tube BSV-29 with a copper anode and scintillation detector NaI (Tl).
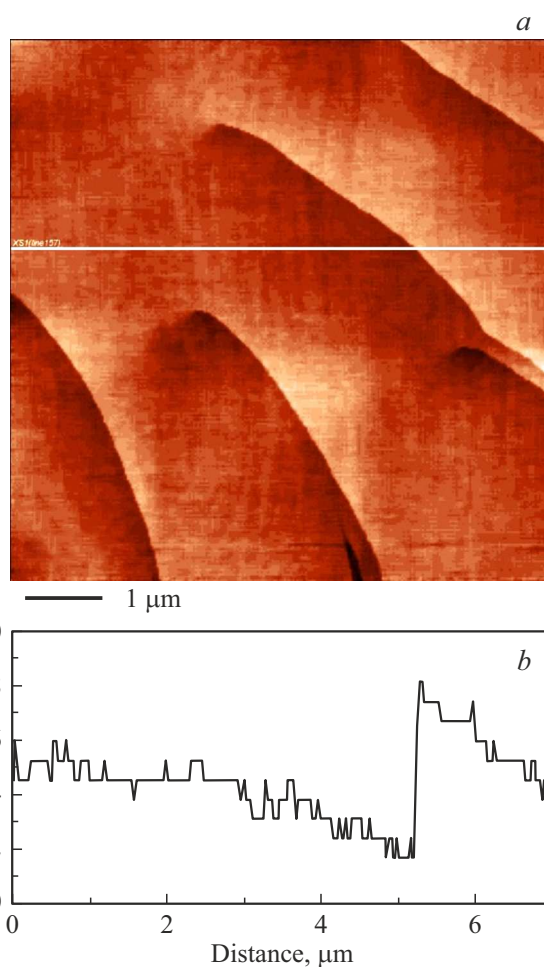
Figure 1. a — AFM image of the (100)β-(Al$_{0.19}$Ga$_{0.81}$)$_2$O$_3$ sample surface; b — relief profile along the white line in the Fig. a.

3. Experimental results and discussion

A number of experiments on the crystal growing [17] were carried out and the inhomogeneity of their cathodoluminscescence was studied. For further experiments the sample with the most inhomogeneous luminescence was selected.

By electron probe microanalysis method the aluminum content in these samples was measured, it was 7.6 at%. It was shown, that in the areas with various luminescence the aluminum content is the same up to experimental error. So the change of cathodoluminescence is not due to the inhomogeneous distribution of aluminum impurities.

Using atomic-force microscopy (AFM) method it was demonstrated, that the crystal surface is atomically smooth and has no relief features, which could be associated with luminescence inhomogeneities. By means of AF method the individual exits of screw dislocations were found (Fig. 1). Thus, it can be assumed, that luminescence inhomogeneity is not related tothe block sample structure, but reflects an inhomogeneous distribution of point defects in the crystal.
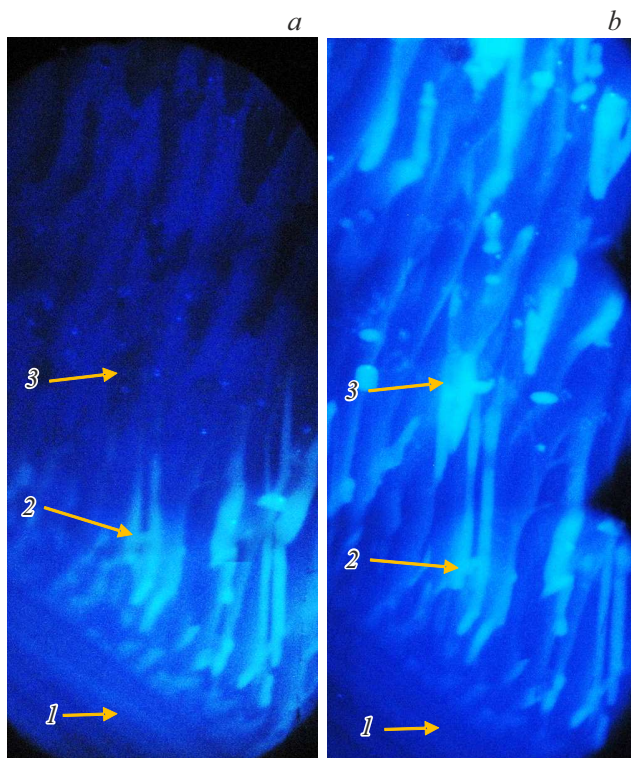
Figure 2. CL image of β-(Al$_{0.19}$Ga$_{0.81}$)$_2$O$_3$ crystal: *a* — before annealing, *b* — after annealing.

CL images of β-(Al$_{0.19}$Ga$_{0.81}$)$_2$O$_3$ crystal were obtained before and after annealing. It is seen, that both in the initial sample, and after the annealing, the areas of various luminescence are observed (Fig. 2, *a*). After the annealing the areas (*1*) and (*2*) marked in Fig. 2, *a*, do not change the luminescence and shapes. However, in the area (*3*) luminescence there is a significant change.

The cathodoluminescence spectra were obtained (Fig. 3) in the areas marked in Fig. 3 before and after annealing. In the region (*1*), the CL spectrum can be approximated by one band (UVB) with the maximum 3.44 eV and a half-width of 0.34 eV. The maximum of the UVB band has a blue shift by 0.3 eV relative to the literature data for Ga$_2$O$_3$, that is explained by an increase in the band gap for (Al$_{0.19}$Ga$_{0.81}$)$_2$O$_3$ solid solution compared to Ga$_2$O$_3$, and accordingly, the shift of the bands associated with own defects, into the blue area. After the annealing in air, the spectrum shape remains the same, and the luminescence intensity increases by 1.5 times. This result is consistent with the literature data [5,6].

In the region (*2*) the CL spectrum consists of two bands with the maxima — 3.44 eV (UVB) and 2.55 eV. We assume that the CL band with a maximum 2.55 eV is GB (2.3 eV) band with the blue shift. The annealing leads to a decrease in the half-width of both bands by $\sim 10\%$ and to an increase in the intensity of both
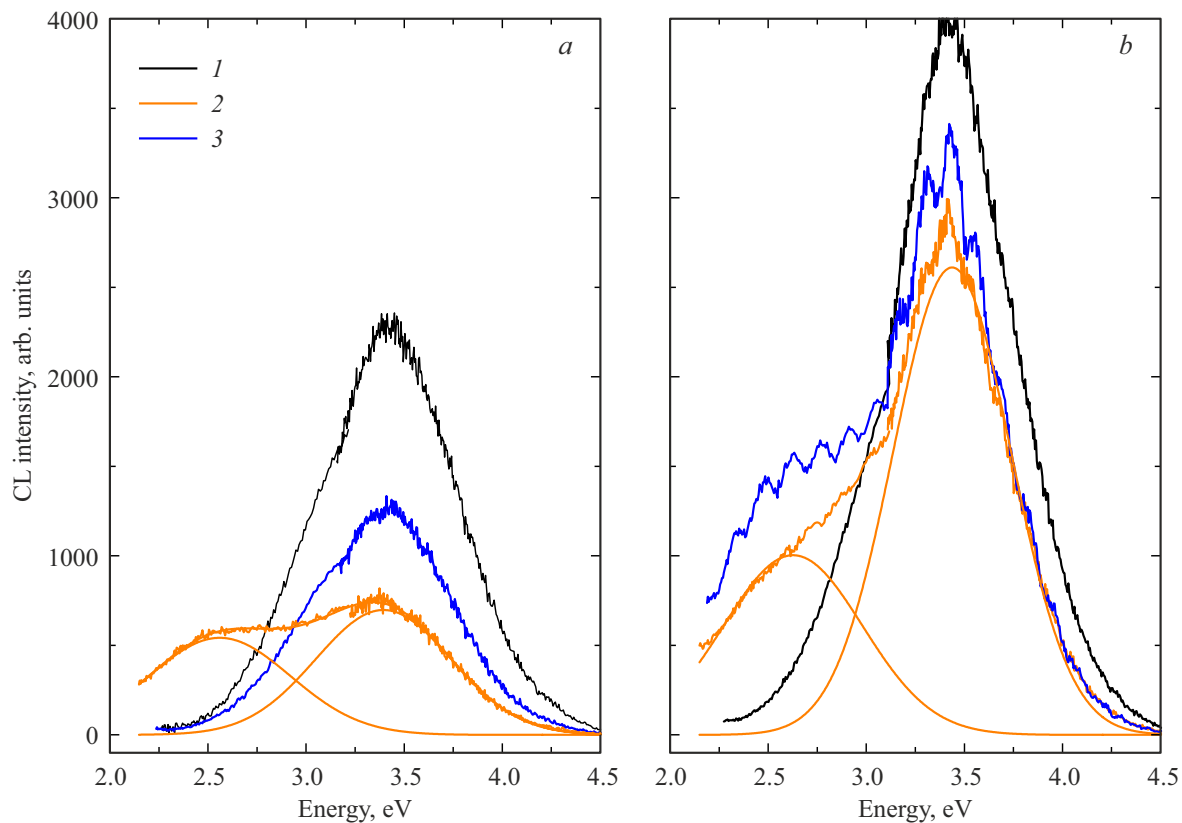

Figure 3. CL spectra of β-(Al$_{0.19}$Ga$_{0.81}$)$_2$O$_3$ crystal: *a* — before annealing, *b* — after annealing in the air, obtained in the areas marked *1, 2* and *3* in Fig. 2. The figure also shows the approximation curves for the spectra obtained in the area (*2*) by the sum of two Gaussian curves.
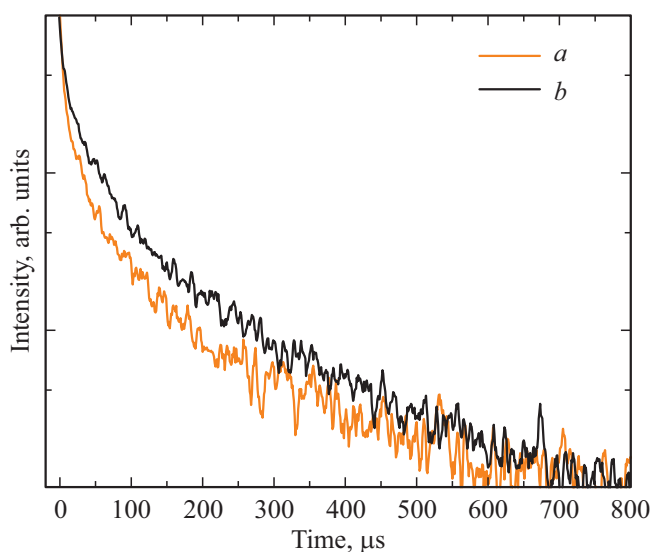
Figure 4. The decay dynamics of the cathodoluminescence band: *a* — areas (*2*) before annealing; *b* — areas (*2*) after the annealing in semilogarithmic scale.

bands, GB intensity increases by 2 times, and UVB — by 3 times.

In the area (*3*) of the initial sample, the spectrum is similar to the region (*1*) spectrum, but has a lower intensity, that indicates a higher probability of nonradiative transitions in these areas. After the annealing the (*3*) region CL spectrum is similar to (*2*) area spectrum after the annealing. However, in this spectrum, the total luminescence intensity increases and an intense GB band appears. The spectrum exhibits periodic oscillations equidistant in wavelengths. These oscillations are associated with the interference of light in a thin layer. Possibly, in this area in the process of annealing the crystal creaming occurred.

We obtained the decay dynamics of the 2.55 eV band of the area (*2*) of the initial sample and area (*2*) and (*3*) of the annealed sample (Fig. 4), in the spectra of which this band was observed. The obtained dynamics were well approximated by the sum of two decaying exponents, characteristic times and intensity ratio are presented in the table. It is seen, that the annealing leads to an increase in the 2.55 eV band decay time and increase of the part of the long component. It shows a decrease in the part of non-radiative recombination due to the defect annealing.

The data obtained allow us to assume, that in (*3*) area, the transformation of the defects associated with non-radiative

Decay times of 2.55 eV band and the ratios of their intensities measured in various sample areas

Area	τ_1 (μs)	I1, %	τ_2 (μs)	I2, %
(*2*) initial	13 ± 1	64	165 ± 5	36
(*2*) after annealing	22 ± 1	57	213 ± 5	23
(*3*) after annealing	22.4 ± 1	61	225 ± 5	39

recombination into luminescent centers with a luminescence maximum of 2.55 eV is observed. Probably, this band is indeed related to the luminescence of gallium vacancies, as was suggested in the paper [11].

4. Conclusion

It was shown, that the contrast of cathodoluminescent image is determined by the change in the intensity and ratio of ultraviolet and green luminescence bands. As no correlations of these properties with composition and topography were found, it can be concluded, that the change in CL spectrum is associated with an inhomogeneous distribution of point defects. The sample annealing led to an increase in the intensity of CL bands in all areas and to the transformation of defects in the sample areas with low intensity. Increasing of intensity after annealing was accompanied by an increase in CL bands decay times. This also testifies a decrease in the concentration of non-radiative recombination centers.

Conflict of interest

The authors declare that they have no conflict of interest.

References

[1] S.J. Pearton, F. Ren, M. Tadjer, J. Kim. J. Appl. Phys., **124**, 220901 (2018).
[2] X. Chen, F. Ren, S. Gu, J. Ye. Photonics Res., **7**, 381 (2019).
[3] S.J. Pearton, J. Yang, P.H. Cary, F. Ren, J. Kim, M.J. Tadjer, M.A. Mastro. Appl. Phys. Rev., **5**, 011301 (2018).
[4] J. Xu, W. Zheng, F. Huang. J. Mater. Chem. C, **7**, 8753 (2019).
[5] T. Harwig, F. Kellendonk, S. Slappendel. J. Phys. Chem. Solids, **39** (6), 675 (1978).
[6] A.I. Kuznetsov, V.N. Abramov, T.V. Uibo. Opt. Spectrosc., **58**, 368 (1985).
[7] L. Binet, D. Gourier. J. Phys. Chem. Solids, **59** (8), 1241 (1998).
[8] V.I. Vasil'tsiv, Ya.M. Zakharko, Ya.I. Prim. Ukr. Fiz. Zh., **33**, 1320 (1988).
[9] O.M. Bordun, B.O. Bordun, I.Yo. Kukharskyy, I.I. Medvid. J. Appl. Spectrosc., **84** (1), 46 (2017).
[10] C. Liu, Y. Berencén, J. Yang, Y. Wei, M. Wang, Y. Yuan, C. Xu, Y. Xie, X. Li, S. Zhou. Semicond. Sci. Technol., **33**, 095022 (2018).
[11] Q.D. Ho, T. Frauenheim, P. Deák. Phys. Rev. B, **97**, 115163 (2018).
[12] T. Harwig, F. Kellendonk. J. Solid State Chem., **24**, 255 (1978).
[13] W. Hua, Sh. Lia, Y. Hua, L. Wana, Sh. Jiaoc, W. Hub, D.N. Talward, Zh.Ch. Fenga, T. Lia, J. Xua, L. Weia, W. Guoe. J. Alloys Compd., **864**, 158765 (2021).

[14] P.N. Butenko, D.I. Panov, A.V. Kremleva, D.A. Zakgeim, A.V. Nashchekin, I.G. Smirnova, D.A. Bauman, A.E. Romanov, V.E. Bougrov. Mater. Phys. Mechanics, **42**, 802 (2019).

[15] D.A. Zakgeym, D.Yu. Panov, V.A. Spiridonov, A.V. Kremleva, A.M. Smirnov, D.A. Bauman, A.E. Romanov, M.A. Odnoblyudov, V.E. Bugrov. Pisma ZhTF, **46** (22), 43 (2020) (in Russian).

[16] M.V. Zamoryanskaya, S.G. Konnikov, A.N. Zamoryanskii. Instrum. Exper. Techn., **47** (4), 477 (2004).

[17] E.V. Ivanova, P.A. Dementev, M.V. Zamoryanskaya, D.A. Zakgeym, D.Yu. Panov, V.A. Spiridonov, A.V. Kremleva, M.A. Odnoblyudov, D.A. Bauman, A.E. Romanov, V.E. Bugrov. FTT, **63**, 4 (421) (in Russian).